Atmospheric Turbulence

Presented to the
University of California, San Diego
Department of Mechanical and Aerospace Engineering
MAE 126A
2/22/2016

Prepared By:
Group EE2
Section A02 (Tuesday PM)
Luis De La Torre
Scott Fuller
Megan Ong
Diana Wu Wong
Stewart Kerr

Abstract:

The CSAT instrument measuring wind speed in three directions, u, v, and w is the primary device in this Atmospheric Turbulence experiment. This device also is able to measure net radiation from solar down welling and upwelling via the Earth's radiation. The environment of the first week of this experiment combined the enclosed atmosphere of EBU II. Here we were surrounded by tall buildings on all sides with only walkways allowing the passing of atmosphere. The solar and the Earth's radiation were quantified by covering the top and bottom side (not simultaneously) of the radiometer. The second taking of data occurred in the large open field directly south of the Jacobs School of Engineering EBU I (32.881224° latitude and -117.235467° longitude). Here, we recorded radiation, wind velocities, and temperatures over approximately twenty minutes. In the first week, we discovered the physical factors that contribute to the CSAT. The second week's radiation is characterized by R_net = 397.0586 Wm^2. We also found u,v, and w when averaged to be 1.4048, .29997, and -.0657 m/s respectively for the Upper CSAT(CSAT 4). The lower CSAT's (CSAT 3) averages were as follows, 1.3461, .2853, and .0077 m/s, respectively. The temperatures for the upper and lower CSAT were 25.0597 °C and 25.4726 °C respectively.

TABLE OF CONTENTS

List of Figures

List of Tables

Introduction

The Atmospheric Boundary Layer (ABL) is the lowest portion of the atmosphere in which we live and breathe from. Consequently, the 1-km-thick layer is the same portion of the atmosphere where all of the gas emissions and exhaust are discharged from[1]. ABL is affected by Atmospheric Turbulence (AT), a small scale small-scaled, irregular air motion processes characterized by winds in different speed and direction, in which comes in two forms: First, in mechanical form in which the friction between the surface of the earth and the wind, resulting a gradient wind field in which the air flow is complex and turbulent created by the atmospheric conditions and the underlying nature of the terrain. Secondly, in thermal form in which the solar radiation heats up the surface and reflects off it. The heat is then mostly absorbed by water vapor, carbon dioxide and other gases causing the greenhouse effect[2].

Both mechanical and thermal forms have great implications on the current problem of air pollution and climate change, as the gas emissions accumulate in the ABL and these same particles cause temperature rise. This process is vital for the transportation of water vapor, air pollutants and, most importantly, energy. Today, scientists and engineers research AT for a variety of application ranging from chemical dispersion of the air pollutants for air quality control to air transport applications. For instance, the National Center of Atmospheric Research has developed an in situ algorithm in order to infer and report turbulence encountered by commercial transport aircraft. This algorithm will predict metric for forecasting purposes, hence reducing communication costs and increasing the safety from the passengers. It is already implemented in 70 Delta Airlines planes and it is projected to be installed in other major airlines in the future[3].

In this experiment, the Campbell Scientific Sonic Anemometer-Thermometers (CSAT) and an NR-LITE radiometer are used to measure the wind speed and temperature of a particular region. The CSAT uses ultrasonic signals in opposite directions to measure the wind speed in 3 different axis from the time of flight. It also measures the temperature using the speed of sound, as it is dependent on air pressure, density and moisture content. Therefore the temperature measured by the CSAT is not the actual

air temperature. The NR-LITE net radiometer performs an algebraic sum of the measured shortwave and longwave radiation. The data from these measurements was analyzed and plotted using MATLAB, in order to gain an understanding on how the solar radiation and air turbulence affects the heat flux and the energy transportation in the atmosphere.

Theory

The net radiation of the Earth is a balance of the energy that is incoming and leaving the surface and atmosphere of the Earth. The Earth's net radiation is balanced by four energy sinks: conduction (G), sensible heat flux (H), latent heat flux (LE), and photosynthesis (P). Conduction is the heat flux caused by a large temperature gradient between the Earth's crust and it's surface. Sensible heat flux is the transfer of heat by convection from the surface of the Earth to the atmosphere. Latent Heat flux is the transfer of moisture from the surface of the Earth to the atmosphere via convection as well. Lastly, photosynthesis is the process by which plant organisms convert incoming solar radiation into energy. by adding these four sinks, the Earth's net radiation can be expressed by the equation:

$$R_{Net} = G + H + LE + P \tag{1}$$

An NR-LITE net radiometer is an instrument used to measure the radiation entering and leaving the Earth's surface and atmosphere in order to determine Rnet. Latent heat flux and photosynthesis can be ignored in the determination of Rnet. Since latent heat flux is a function of specific humidity and humidity is minimal in San Diego's mild climate, latent heat flux can be neglected. In the case of photosynthesis, the amount of solar radiation that is consumed by plant organisms is relatively small and can be neglected as well. Conduction is evaluated after determining sensible heat flux, which is determined by the equation:

$$H = \rho_a c_p \overline{w'T'} \tag{2}$$

where ρais the density of air, cpis the specific heat of air, and w'T' is the convective heat flux. w and T represent vertical wind velocity and temperature at a certain instance in time, respectively. In order to solve for turbulent fluctuations of vertical wind velocity, w', and temperature, T', the following equations may be used:

$$w = \overline{w} + w' \tag{3}$$

$$T = \overline{T} + T' \tag{4}$$

where w and T represent the average vertical wind velocity and average temperature, respectively.

Vertical convective heat flux is measured through the use of sonic anemometers via the eddy covariance method which measures vertical heat fluxes found within the atmospheric boundary layer. The anemometers consist of a pair of transducers that measure the vertical wind velocities and temperature between the pair at a high resolution. This high resolution is determined by the path length between the pair and makes these instruments well suited for taking measurements of turbulence.

Vertical heat flux measurements play a vital role in understanding the stability of the atmosphere. Atmospheric stability is characterized by the atmospheric resistance to vertical motion. During the day, eddies transport warmer buoyant air upwards while transporting colder, denser air towards the surface. This results in a positive heat flux indicating atmospheric instability. On the contrary, during the night, eddies move the colder air upwards and transports the warmer air down to the surface resulting in a negative heat flux and indicating stable atmospheric conditions.

Unstable atmospheric conditions are mainly the result of a deep atmospheric surface layer and boundary layer. These deep layers are the result of large eddies caused by a wind gradient starting at the surface of the earth. As the height increases, the wind velocity also increases as a result of the no-slip boundary condition. The mean velocity profile can be best described by the logarithmic equation that provides a visual of the size of the boundary layer from the surface of the Earth to the height of the boundary layer. The mean velocity profile is computed through the equation:

$$\frac{\overline{u(z)}}{u^*} = \frac{1}{k} ln(\frac{z}{z_0}) \tag{5}$$

where u(z) is the average horizontal velocity, u* is the friction velocity, k is known as the von Karman constant and has a value of 0.4, z is the height above the surface, and z0 is known as the roughness length which is equal to the 1/10th height of the obstacles. The friction velocity is obtained through the equation:

$$u^* = [(\overline{u'w'})^2 + (\overline{v'w'})^2]^{1/4} \tag{6}$$

where u' and v' are the turbulent fluctuations of the horizontal velocities in the x and y directions, respectively. When friction velocity increases, atmospheric turbulence and large eddies will also increase, thus resulting in unstable atmospheric conditions.

Experimental Procedure

Two Campbell Scientific sonic anemometer-thermometers (CSAT) and an NR-LITE net radiometer are used to accurately measure atmospheric turbulence and net radiation. The CSAT instruments consist of an anemometer head, anemometer mount, SDM and power wires, and the CSAT electronic box. Each anemometer was mounted on the same side of the two long horizontal arms of the tripod. Each anemometer head was mounted carefully on their respective mounts and was held by block. The bubble level indicator located on the upside of the anemometer was used to level anemometer head onto the mount. The horizontal arm was then pointed into the prevailing wind. The CSAT with SDM address 3 was mounted 1 meter above the ground in the lower position, the CSAT with SDM address 4 was mounted 1.7 meters above the ground in the upper position. The wire from each anemometer head was connected to the 'transducer head' of their respective electronic box, and the SDM and power wires were then connected to the '+12V SDM' port of the electronic box. Next, the CSAT instruments were oriented at 238° W.

The net radiometer had a calibration factor of 14.1VW-1m-2and was mounted on the upper horizontal arm of the tripod on the opposite side of the CSAT. The net radiometer was then leveled using the bubble level indicator located on the upperside of the sensor. Once both the CSAT and net radiometer were mounted and leveled, the SDM and differential ports were located on the Campbell Scientific CR1000 datalogger. Following the wiring instructions for CSAT, the SDM and the power wires were connected to the SDM ports. The wires from the net radiometer were then connected to the differential ports on the datalogger following the wiring instruction for the net radiometer. Next, the datalogger was connected to the battery.

After the datalogger was connected to the battery, it was connected to the laptop using the RS-232 and USB connection wire in order to begin data collection. Upon entering the Loggernet program, we navigated to 'Main' and then to 'connect'. We then highlighted the CR1000_mae126a in the stations menu and connected. Once we successfully connected, the clock of the datalogger was calibrated by clicking the set button in the clocks block. The datalogger program was then sent by clicking 'send' in the program block and the file was stored on the desktop of the laptop. 'Table 1' in the Table Monitor: Passive Monitoring block was selected in order to check our data.

Next, the airflow was observed in the EBU II quad. Group members then blew air to the CSAT in order to observe changes in the readings. Then a group member covered the upper side of the net radiometer with their hand and we observed how the readings were changing. The lower side of the net radiometer was also covered by hand and changes in the readings were also noted. After this was done, the data was transferred onto a USB drive by clicking 'collect' in the menu. The data that we obtained was then read on MATLAB using a read_file.m script.

We then proceeded to measure the atmospheric turbulence at an open location in Warren court at 32°52'52"Nand 117°14'7"W. We made sure to section the area where our equipment was located to prevent any passerby from disrupting our data collection and chose a relatively flat region in Warren court so that the orientation of the CSAT was not disrupted. After these preventive measures were made, data was collected for 20 minutes with a 10 Hz frequency which resulted in 12,000 samples. Once the measurements were recorded, the sensors were dismounted carefully.

Next, the data was downloaded and MATLAB was used to evaluate the data obtained. Using MATLAB, we wrote scripts to plot the entire time series of U,V,W,T using five subplots in order to compute mean U,V,W.T and plot the turbulent fluctuations U',V',W', and T'. MATLAB scripts were also written to plot the time series of u'w' and w'T'. Lastly, we computed the covariance and correlation coefficients between U and W, and W and T, the velocity profile in the log layer of the atmosphere, the mean velocity estimated for the height of other CSAT, and all possible terms of the surface energy

balance.

Results

The first part of this experiment was conducted, at UCSD in the EBUII courtyard, to determine the response the CSAT readings would have to various atmospheric changes or stimuli. The responses were observed and manipulated to note the proportionality between them and the output responses. When air was blown into the sensors, for example, the readings showed a significant spike in the magnitude of velocities in all three directions. The u velocity, that associated with the x direction given a Cartesian coordinate system, had a positive spike; while the v and w velocities, those associated with the y and z directions of a Cartesian coordinate system, respectively, showed a negative spike. To understand the operational mechanics of the net radiometer, the top and bottom of the radiometer were covered and uncovered and the corresponding changes in radiation, or R_{net}, were observed. R_{net} is the difference between the incoming solar radiation and the radiation emitted from the earth's surface. Covering the upper side of the net radiometer resulted in a drop in the signal output as was expected from a reduction in incoming solar radiation. Covering the lower side of the radiometer, on the other hand, showed an increase in the net radiation as there was a decreased loss due to emissions.

The second part of the experiment was conducted between 1:05:00 PM to 1:25:00 PM on February 9, 2016. The experiment was performed at 32.881224° latitude and -117.235467° longitude. The CSATs were pointed towards the Geisel Library at approximately 240° SW. The measurements of the readings from CSAT 3 and CSAT 4 were summarized in Figure 1; including the three dimensional velocities, the temperature, and the net radiation for the time series.

During the time that this experiment was conducted, DEMROES reported an average incoming solar radiation of approximately 730 ± 36.5 $Wm2$[4]; the CR1000 displayed an average net radiation of 397.0586 ± 30 $Wm2$throughout the same time frame. According to Equation 1, the net radiation is equivalent to the sum of the sensible heat flux and the conduction. Therefore, the outgoing radiation was 332.9414 ± 47.247 $Wm2$. According to Equation 2 and tabulated values for the density and specific heat of air at 25 °C, the sensible heat flux, H, was calculated to be 25.2933 ± 1.572 Wm2for CSAT 3[5]. The

covariance values for the velocity in the x direction and the z direction (u and w) were both slightly positive for CSAT 3 and CSAT 4. CSAT 3 had a covariance value of 0.3050 and CSAT 4 had a covariance value of 0.3013. There was a positive relationship for the covariance values of the vertical velocities (w) for both CSAT 3 and 4 in relation to the temperatures; this value of 0.0457 for CSAT 3 and 0.0603 for CSAT 4 corresponds to a positive linear relationship between the temperature of each CSAT and the vertical velocity of each CSAT, respectively. Table 1 shows a breakdown of the mean measurements for the velocities, and temperatures for both anemometers, as well as the net radiation as a whole. The correlation coefficients for the temperature in relation to the vertical velocity was 0.4261 for CSAT 3 and 0.3671 for CSAT 4. The correlation coefficients for the horizontal velocity in relation to the vertical velocity was -0.0174 for CSAT 3 and -0.0409 for CSAT 4. The relative relationships between the velocities and the temperatures can be determined from these values. The values of the covariance and correlation coefficients can be found in Table 2. The turbulent momentum flux (u'w') and the sensible heat flux (w'T') can also be analyzed from their respective time series found in Figures 6 and 7.

Table 1: Mean values for three-dimensional velocity, temperature, and net radiation for CSAT 3 and 4

	CSAT 3	CSAT 4
U (m/s)	1.3461	1.4048
V (m/s)	0.2853	0.2997
W (m/s)	0.0077	-0.0657
T (°C)	25.4726	25.0597
Rnet	397.0586	

Table 2: Covariance and correlation coefficients for CSAT 3 and 4

	CSAT 3	CSAT 4
cov(u,w)	0.3050	0.3013
Cov(w,T)	0.0457	0.0603
R(u,w)	-0.0174	-0.0409
R(w,T)	0.4261	0.4124

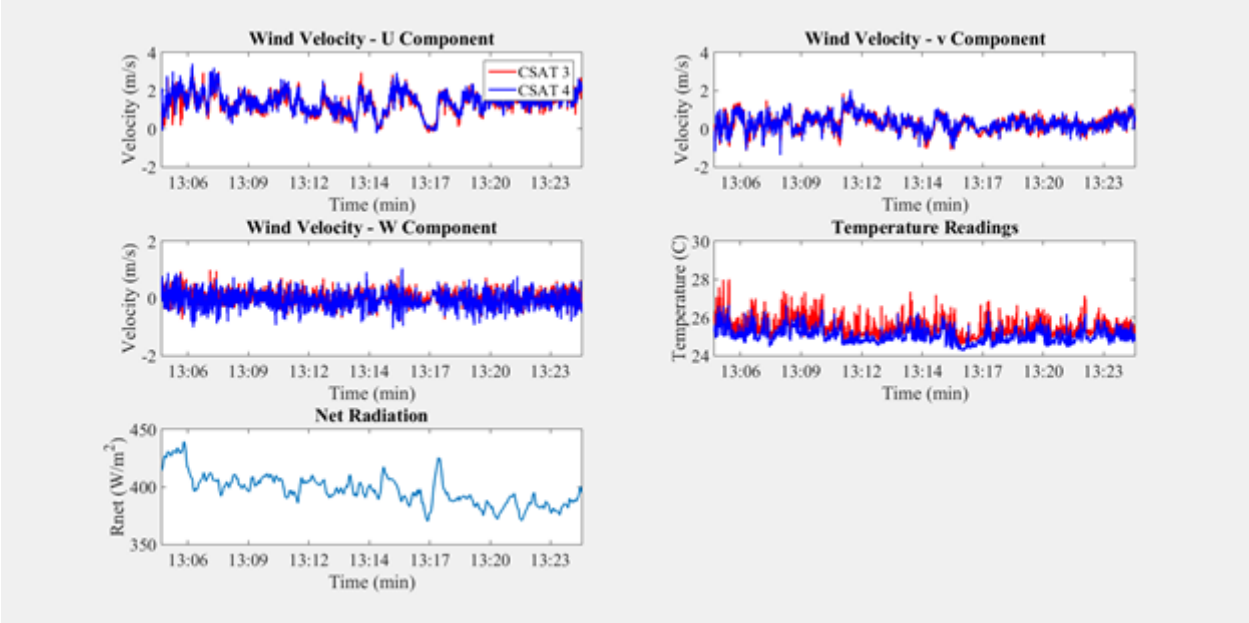

Figure 1: Velocity, Temperature, and Radiation Time series for CSAT 3 and 4

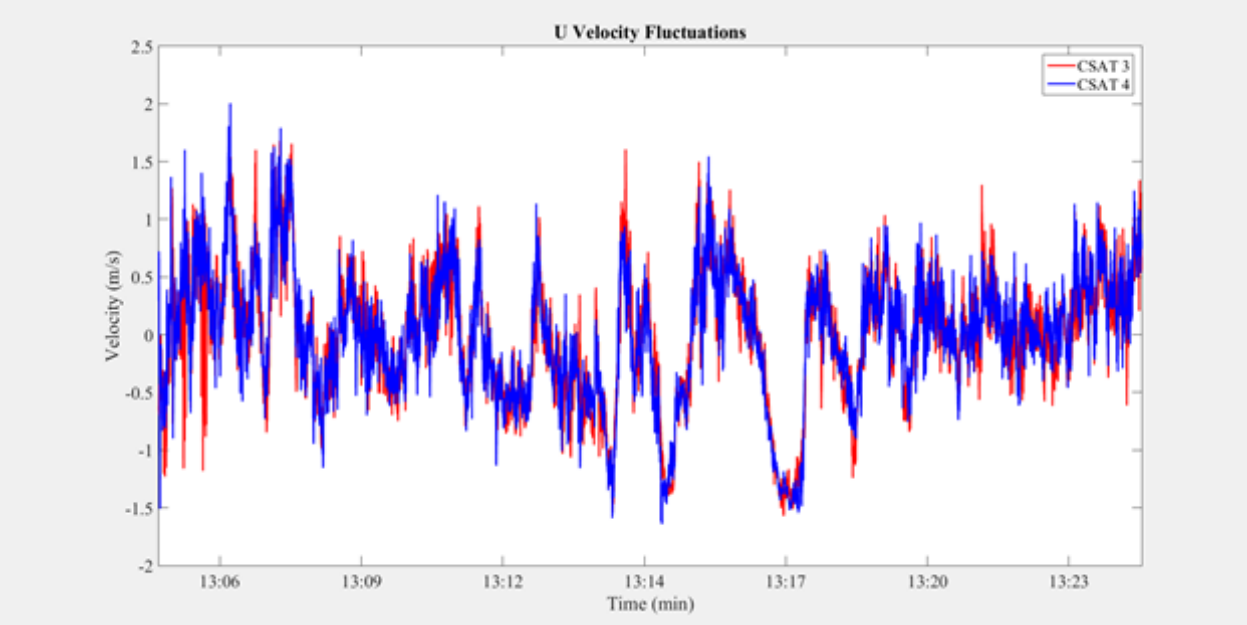

Figure 2: Time series of X-directional Velocity Fluctuations for CSAT 3 and 4

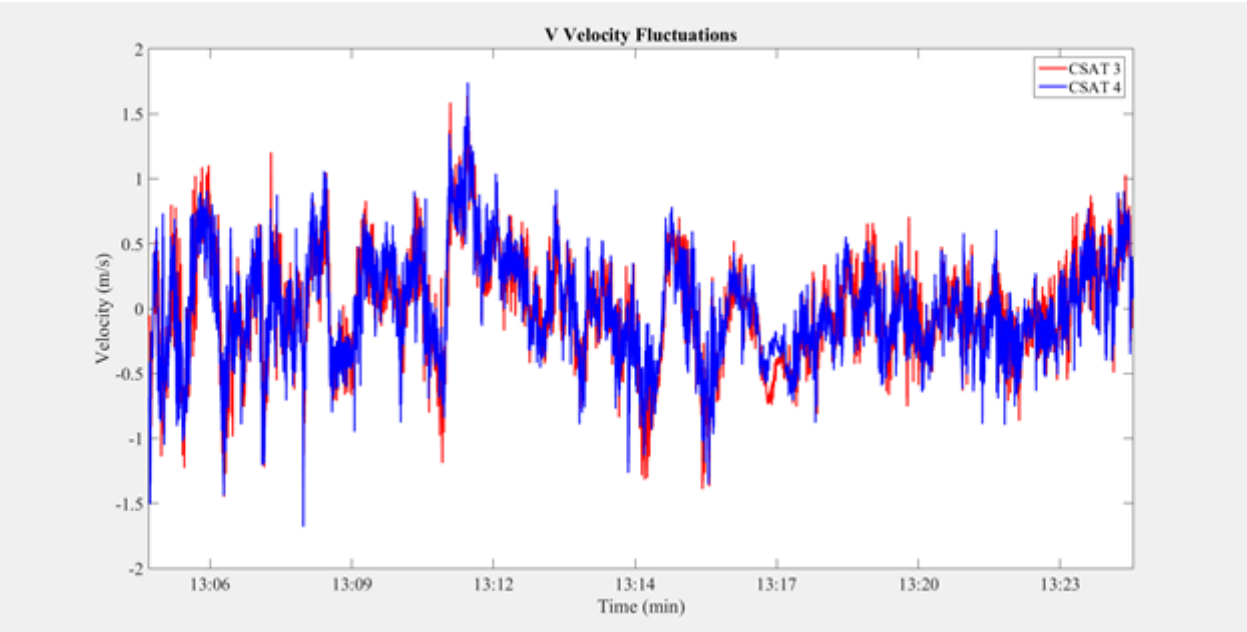

Figure 3: Times series of Y-directional Velocity Fluctuations for CSAT 3 and 4

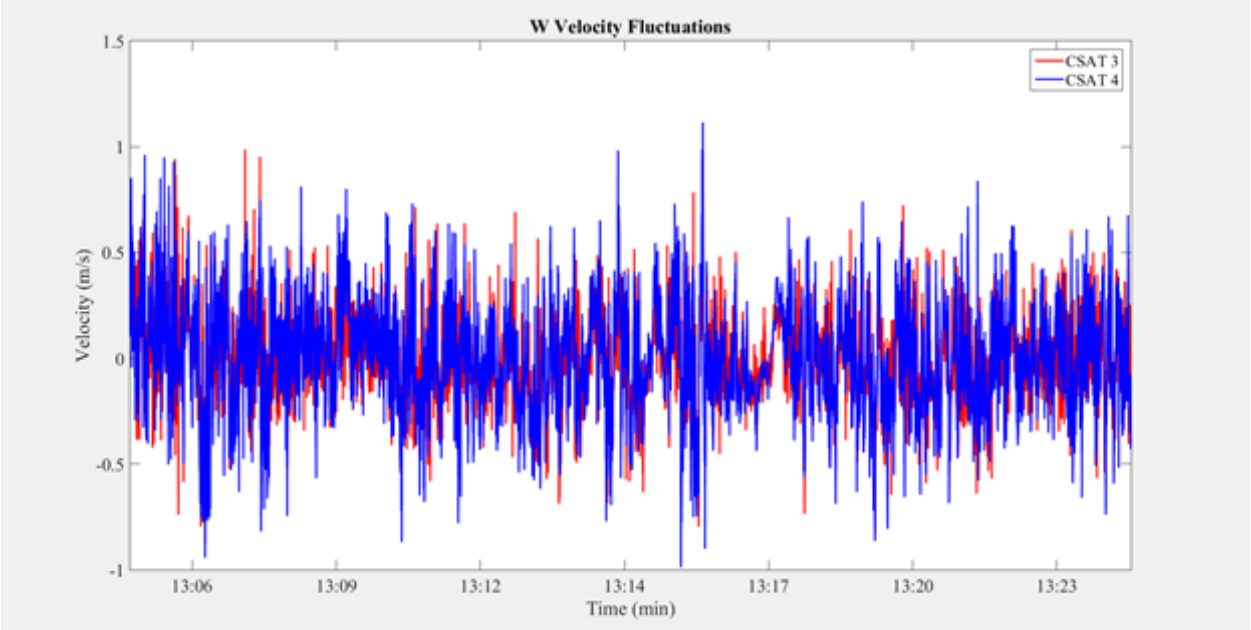

Figure 4: Times series of Z-directional Velocity Fluctuations for CSAT 3 and 4

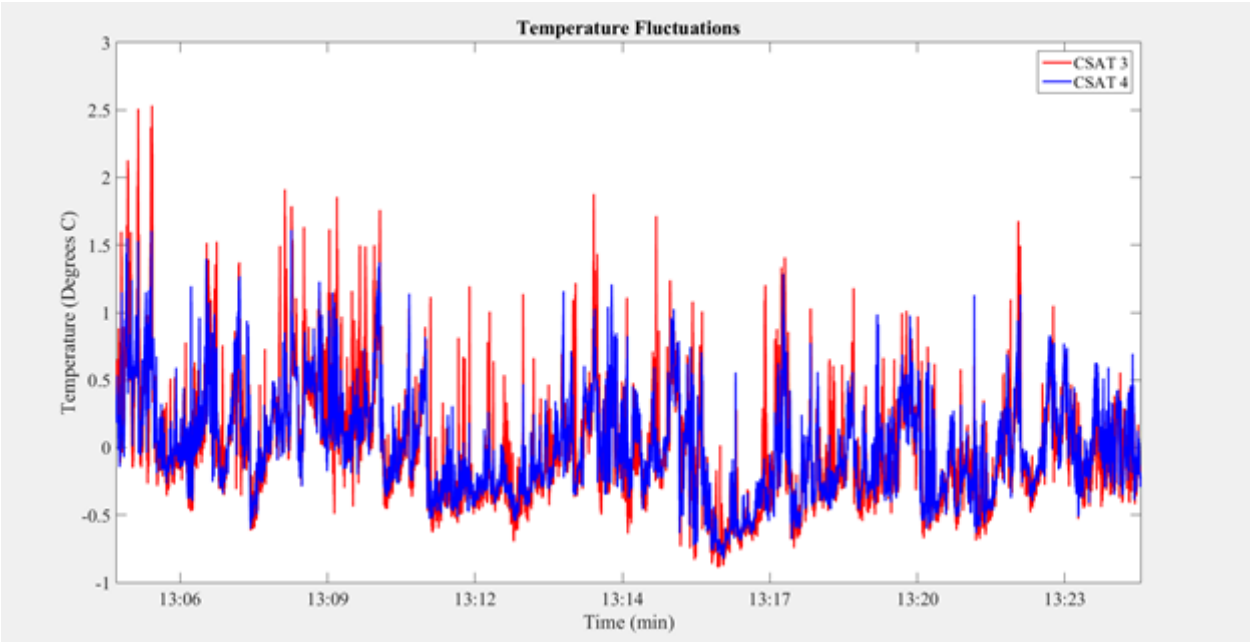

Figure 5: Times series of Temperature Fluctuations for CSAT 3 and 4

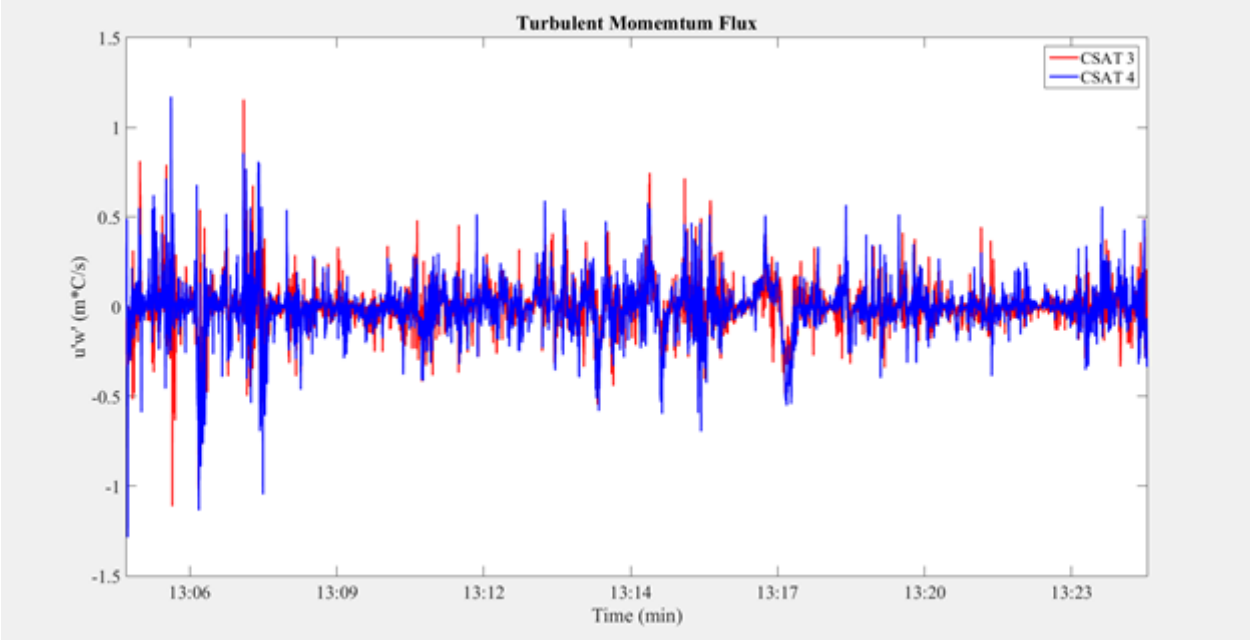

Figure 6: Time series of Turbulent Momentum Flux for CSAT 3 and 4

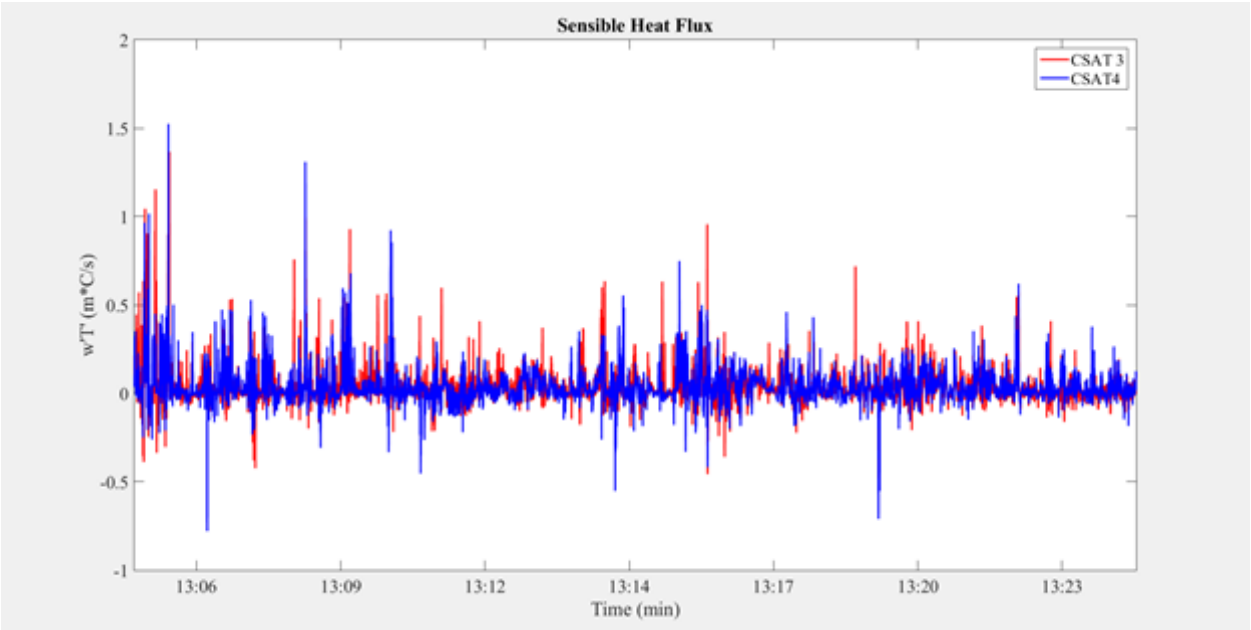

Figure 7: Time series of Sensible Heat Flux

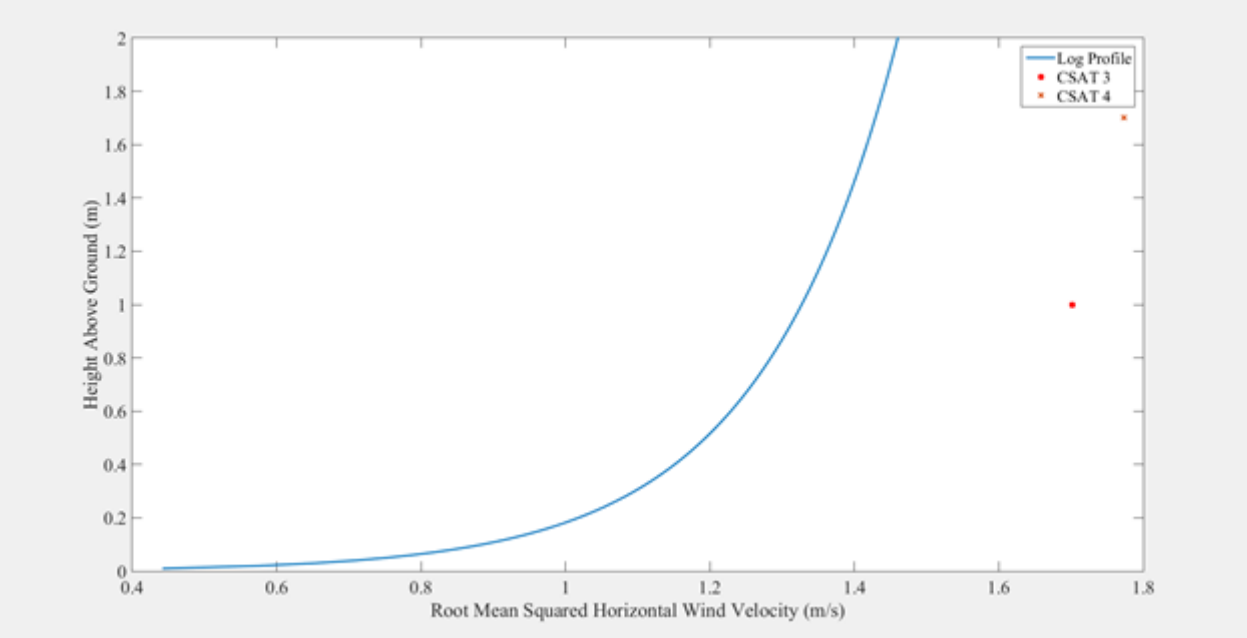

Figure 8: Log Layer Velocity Profile for Calculations of Root Mean Squared Horizontal Wind Velocity

Error Analysis

The experiment's main sources of discrepancy comes from the systematic setup of the devices as well as the potential inherent flaw of the instruments. First, the devices were not set up at a flat ground, the slope was about 10°-15° tilted. During Week 1, the devices were placed within the patio of the Jacobs School of Engineering Building II facing Geisel Library with 270° West on an uneven, concave up, ground. During Week 2, the devices were set at the Warren Mall near the Jacobs School of Engineering Building I, again, facing 270° West facing the Geisel Library on a 15°-20°slope tilting East. The offset reduces the precision when measuring the wind speed U, V and W directions since the velocities from each direction would not perfectly correspond to the x, y and z direction. Nevertheless, the CSAT contains a bubble level indicator to help level the instrument and reduce the chance for discrepancy. The NR-LITE, however, does not have a bubble level indicator and it is placed according to the setup. According to the CSAT product website, measurement resolutions are 1 mm/s rms for both ux and uy; 0.5 mm/s rms for uz and wind direction 0.06° rms. The corresponding offset errors are smaller than 8.0 cm/s (ux, uy) and 4.0 cm/s (uz) respectively. The gain error in the measured incoming radiation is approximately 5%.

Uncertainties noted in this experiment were calculated from error propagation methods. For the net radiation calculations, an error of 5% was used which corresponds to an error of $\pm 36.5 \frac{W}{m^2}$. The error for the net radiation was taken as $\pm 30 \frac{W}{m^2}$ based on the error in the net radiometer as described by the manufacturer[3].Based on this, the outgoing radiation emissions had an error of $\delta Rout = \sqrt{(\delta Rin)^2 + (\delta Rnet)^2} = \pm 47.247 \frac{W}{m^2}$. The uncertainty in the heat flux, H, was calculated to be $\delta H = H\sqrt{(\frac{\delta w}{w})^2 + (\frac{\delta \gamma}{\gamma})^2} = \pm 1.572 \frac{W}{m^2}$.

Discussion

Week 1: Installation and data logging of atmospheric sensors

Using the datalogger interface the airflow in the lab could be observed via the graph monitor. As discussed in results, when air was blown onto the sensors the readings displayed a positive spike in the u velocity and a negative response in the v and w velocities. Additionally when the net radiometer was covered from above and below, the readings of R_{net} changed due to a reduction for incoming radiation.

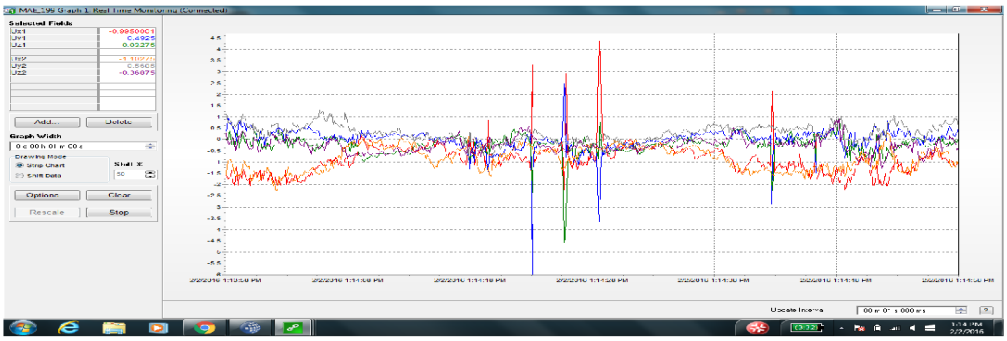

Velocities when air was blown at the sensors

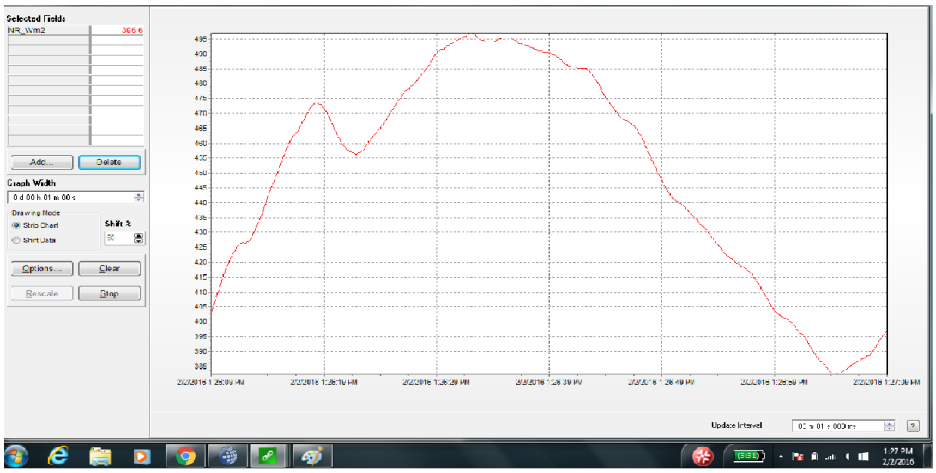

Radiometer covered from below

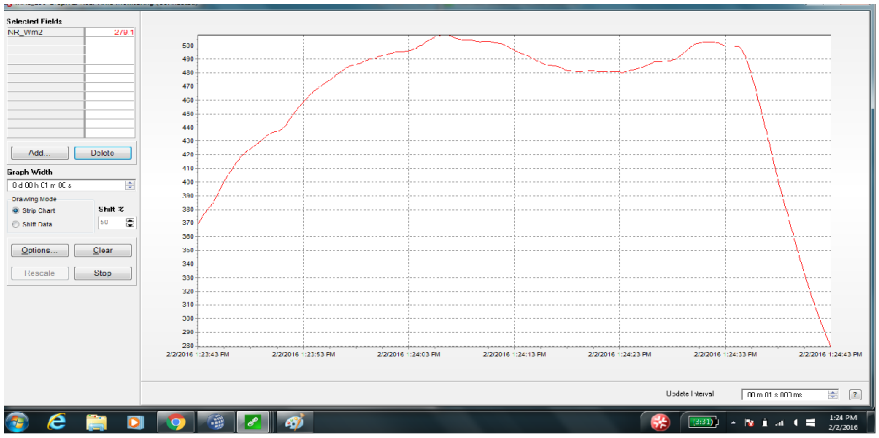

Radiometer covered from above

Week 2: Measure Atmospheric Turbulence

During week 2 the atmospheric turbulence trends were further analyzed by plotting the data collected on February 9, 2016. From the five subplots of the u,v,w, temperature, and net radiation, Figure 1, it can be seen that the flow is turbulent due to the heating the ground. This causes the lapse rate to increase which then then encourages instabilities which increase the turbulence in air. Additionally comparing the trends of the wind velocities, the u velocity had a higher mean value, 1.3461 m/s and 1.4048 m/s, than either the v or w velocities. This is likely due to the sea breeze coming from the west as

well as high buildings (Jacobs Hall) blocking the majority of the winds coming from the north. Both the u and v velocities fluctuated around the same magnitude throughout the experiment, between -2m/s and 2 m/s, and with about the same frequency. However, the w component of the wind velocity remained much closer to 0 m/s but oscillated at a higher frequency. This was a result of the vertical movement of air particles due to heating rather than wind. As the sun heats the earth's surface, the temperature of the ground rises. This warmer land then heats the air near the surface, creating a temperature gradient and causing an upward draft as the warm air rises. This temperature gradient is confirmed by the average temperature readings from the CSAT. The lower CSAT average 25.4726 °C and the upper CSAT average 25.0597 °C. Visually, the resulting updraft is seen as a positive w velocity. This updraft also creates an area of low pressure causing colder air to fill the space. As concrete has a low specific heat, around 0.2 kcal/kg·C, the ground during the experiment took less solar radiation to increase the temperature of the ground and subsequently the air.

When plotting the fluctuation in the velocities, u',v', and w' similar conclusions can be drawn. The fluctuation of the velocity in the x direction varies the most, followed closely by the fluctuation in the y direction. Both u' and v' fluctuate with comparable frequency while the fluctuations in the z direction vary less than the x and y direction but at a much higher frequency. As the air is turbulent and not a consistent flow all day, it is expected that there would be non zero values for T', u', v', and w' .

The covariance of any two variables is a measure of how much the variables change together. When the covariance is positive, then there is a positive correlation between the variables. If the covariance is negative then there tends to be a negative relationship between the variables. The covariance of T and w, cov(T,w), physically represents the dependence of temperature and the z velocity. If this dependence exist, it would confirm there is a convective heat flux. Cov(T,w) was calculated to be 0.0457 for CSAT 3 and 0.0603 for CSAT 4. These positive covariance shows that an increase in temperature causes an updraft of air and thus confirms that a convective heat flux is occurring.

Similarly plotting w'T' against time, in Figure 7, the convective heat flux and similarly sensible can be visualized. Sensible heat flux is the process in which energy is transferred from the Earth's surface

to the atmosphere by conduction and convection. When w'T' is larger positive the boundary layer is unstable leading to larger eddies. Using equation 2 the sensible heat flux was calculated to be 25.2933 ± 1.572 W/m^2.

The correlation coefficient of two variables is the covariance divided by the product of each variable's standard deviation. These values are standardized and the closer the coefficient is to 1 the more correlated the variables are to each other. The correlation between temperature and w, r(T,w), was found to be 0.4261 for CSAT and 0.4124 for CSAT 4. These positive values indicate that w and T are linearly dependent. The correlation between u and w, r(u,w), was -0.0174 for CSAT 3 and -0.0409 for CSAT. These negative values show that they are inversely dependent. Physically this value describes what fraction of the turbulent motion is resulting in a turbulent this is expected as the increase in mixing in the boundary layer results in a decrease in the turbulent diffusion of momentum.

The average velocity can be illustrated by Figure 8 which depicts a log layer horizontal velocity profile. Theoretically the average wind velocities for CSAT 3 and CSAT 4 were calculated to be 1.3247 m/s and 1.4316 m/s, respectively. However using the measured average velocities measured were 1.6909 m/s and 1.7735 m/s. This discrepancy may have been a result of the assumption that there were neutral atmospheric conditions, which resulted in neglecting buoyancy effects. This discrepancy could be also a result of an incorrect estimate of the surface roughness; a factor which determines the Reynold's number of the incoming flow and also is a factor in the way that the velocity boundary layer develops. Because the theoretical log layer develops inversely proportional to the surface roughness, even a small change in its magnitude could result in a significant change in the boundary layer; therefore, resulting in a significant change in the expected velocities for each CSAT.

The average net radiation was found to be 397.0586 ± 30 W/m^2 . Using this value along with equation 1, the surface energy balance can be analyzed. Using standard values for density and specific heat, along with calculating the conduction term as a function of the thermal conductivity of air, the sensible heat was evaluated to be 25.2933 ± 1.572. The ratio of sensible heat, or convection, to net

radiation is 6.4%; therefore, it can be determined that the convection played a relatively small role in the surface energy balance for this experiment on this day. This could be a result of the relatively cooler weather leading up to the day of the experiment while the actual day of the experiment was slightly warmer than the previous few weeks. Latent heat could not be evaluated for this experiment without more knowledge of the specific humidity of the local air. Without infiltration or runoff, the only remaining term in the surface energy balance is photosynthesis; and, as the experiment was conducted near grass and in an area with a relatively large amount of trees, it can be expected that photosynthesis would play a significant role in the energy balance. Photosynthesis effectively limits the amount of radiation emitted by the surface as some is absorbed for this process. This leaves the sum of conduction and photosynthesis to be 371.7653 ± 31.572 $\frac{W}{m^2}$.

During the installation of CSAT, the CSAT must be aligned with the mean wind to ensure that the readings of the vertical fluctuation are not affected by the x and z components of velocity. The experimental mean w velocity was 0.0077m/s for CSAT 3 and -0.0657m/s for CSAT 4 and not zero therefore our CSATs were not exactly aligned which will result in errors in estimating mean wind speeds and fluxes the first part of this experiment, the characteristics of the thermal plume were determined by examining the differences in temperatures and densities between the cold water in tank and the hot water that was injected by the pump. After calibrating the pump, we calculated the linear fit equation y=0.786x+1.2575 which established that the volume flow rate and the pump rotational rate were directly proportional to each other.

Conclusion

The purpose in this experiment was to study the atmospheric turbulence through the analysis of radiation, velocity and temperature. We found that the measures of net radiation were positive. This leads us to conclude that the incoming solar radiation was greater than the outgoing infrared radiation from the Earth. The convective heat flux shows us from the covariance between T and w as they are relatively low. We can conclude that the air nearest the Earth can be considered turbulent due to the temperature and velocity fluxes. From the components u, T and w, it is shown that they are correlated as all of the covariance's are positive. This demonstrates that a change in one variable caused changes to the others. Z direction velocity played a role in the rise of heat since it is moving vertically which caused turbulence in this layer. Overall, it was calculated that such instabilities can be considered negligible, and in a greater reach, it is concluded that the layer closest to the Earth is turbulent, but stable. With that, it is shown that wind velocity trends increasingly with the positive Z direction.

Appendix and Raw Data

MATLAB CODE:

```
set(0, 'defaultaxesfontsize', 20);
set(0, 'defaultlinelinewidth', 2);
set(0, 'defaultaxesfontname', 'Times New Roman');
clear; close all;
%------------------------inputs-----------------------------------------------
file_path='C:\Users\s2kerr\Desktop'; % PLEASE ENTER YOUR FILE PATH
file_name='MAE126A_Week_2_AT'; % PLEASE ENTER YOUR FILE NAME
%------------------------read the datalogger file-------------------------
%Timestring --> Time in string format
%Trash --> Sample number
%Batteryvolt --> Voltage of Battery (V)
%Rnet --> Net radiation from NR-LITE radiometer (W/m2)
%Sonic1 --> Lower CSAT (first column->u(m/s), second column->v(m/s),
%                       third column->w(m/s), foruth column->T(0C))
%Sonic2 --> Upper CSAT (same column definition as Sonic1)
[Timestring, Trash, Batteryvolt, Rnet, Sonic1(:,1),
Sonic1(:,2),Sonic1(:,3),Sonic1(:,4), Sonic2(:,1), Sonic2(:,2),
Sonic2(:,3),Sonic2(:,4)]
=textread(strcat(file_path,file_name),'%23c%u%f%f%f%f%f%f%f%f%f%f','delimiter
',',','headerlines',4);
%---------------------conversion of time-----------------------------------
% quality control of time string
Timestring(Timestring(:,22)==',',:) =...
      strcat(Timestring(Timestring(:,22)==',',1:20), '.0"');
Timestring(:,1) = [];
yr = str2num(Timestring(:,1:4)); %#ok<*ST2NM>
```

```
mo = str2num(Timestring(:,6:7));

dy = str2num(Timestring(:,9:10));

hr = str2num(Timestring(:,12:13));

mi = str2num(Timestring(:,15:16));

sc = str2num(Timestring(:,18:21));

Time = datenum(yr, mo, dy, hr, mi, sc); % time conversion

%Subplots:

%Subplot 1: U

subplot(3,2,1)

plot(Time,Sonic1(:,1),'r')

xlim([Time(1) Time(end)])

datetick('x','HH:MM','keeplimits','keepticks')

hold on

plot(Time,Sonic2(:,1),'b')

xlim([Time(1) Time(end)])

datetick('x','HH:MM','keeplimits','keepticks')

hold off

title('Wind Velocity - U Component')

xlabel('Time (min)')

ylabel('Velocity (m/s)')

legend('CSAT 3','CSAT 4')

%Subplot 2: V

subplot(3,2,2)

plot(Time,Sonic1(:,2),'r')

xlim([Time(1) Time(end)])

datetick('x','HH:MM','keeplimits','keepticks')

hold on

plot(Time,Sonic2(:,2),'b')

xlim([Time(1) Time(end)])
```

```
datetick('x','HH:MM','keeplimits','keepticks')
hold off
title('Wind Velocity - v Component')
xlabel('Time (min)')
ylabel('Velocity (m/s)')
%Subplot 3: W
subplot(3,2,3)
plot(Time,Sonic1(:,3),'r')
xlim([Time(1) Time(end)])
datetick('x','HH:MM','keeplimits','keepticks')
hold on
plot(Time,Sonic2(:,3),'b')
xlim([Time(1) Time(end)])
datetick('x','HH:MM','keeplimits','keepticks')
hold off
title('Wind Velocity - W Component')
xlabel('Time (min)')
ylabel('Velocity (m/s)')
%Subplot 4: T
subplot(3,2,4)
plot(Time,Sonic1(:,4),'r')
xlim([Time(1) Time(end)])
datetick('x','HH:MM','keeplimits','keepticks')
hold on
plot(Time,Sonic2(:,4),'b')
xlim([Time(1) Time(end)])
datetick('x','HH:MM','keeplimits','keepticks')
hold off
title('Temperature Readings')
```

```
xlabel('Time (min)')

ylabel('Temperature (C)')

%Subplot 5: Rnet

subplot(3,2,5)

plot(Time,Rnet)

xlim([Time(1) Time(end)])

datetick('x','HH:MM','keeplimits','keepticks')

title('Net Radiation')

xlabel('Time (min)')

ylabel('Rnet (W/m^2)')

%Calculate averages for U,V,W,T,and Rnet

U1_avgerage = mean(Sonic1(:,1));

U2_avgerage = mean(Sonic2(:,1));

V1_avgerage = mean(Sonic1(:,2));

V2_avgerage = mean(Sonic2(:,2));

W1_avgerage = mean(Sonic1(:,3));

W2_avgerage = mean(Sonic2(:,3));

T1_avgerage = mean(Sonic1(:,4));

T2_avgerage = mean(Sonic2(:,4));

Rnet_avgerage = mean(Rnet);

%calculate fluctuations for U,V,W,T, and Rnet

U1_fluctuation = Sonic1(:,1) - repmat(U1_avgerage,14188,1);

U2_fluctuation = Sonic2(:,1) - repmat(U2_avgerage,14188,1);

V1_fluctuation = Sonic1(:,2) - repmat(V1_avgerage,14188,1);

V2_fluctuation = Sonic2(:,2) - repmat(V2_avgerage,14188,1);

W1_fluctuation = Sonic1(:,3) - repmat(W1_avgerage,14188,1);

W2_fluctuation = Sonic2(:,3) - repmat(W2_avgerage,14188,1);

T1_fluctuation = Sonic1(:,4) - repmat(T1_avgerage,14188,1);

T2_fluctuation = Sonic2(:,4) - repmat(T2_avgerage,14188,1);
```

```
Rnet_fluctuation = Rnet - repmat(Rnet_avgerage,14188,1);
%Plot fluctuations for U
Fig.(2);
plot(Time,U1_fluctuation,'r')
xlim([Time(1) Time(end)])
datetick('x','HH:MM','keeplimits','keepticks')
hold on
plot(Time,U2_fluctuation,'b')
xlim([Time(1) Time(end)])
datetick('x','HH:MM','keeplimits','keepticks')
hold off
title('U Velocity Fluctuations')
xlabel('Time (min)')
ylabel('Velocity (m/s)')
legend('CSAT 3','CSAT 4')
%Plot fluctuations for V
Fig.(3);
plot(Time,V1_fluctuation,'r')
xlim([Time(1) Time(end)])
datetick('x','HH:MM','keeplimits','keepticks')
hold on
plot(Time,V2_fluctuation,'b')
xlim([Time(1) Time(end)])
datetick('x','HH:MM','keeplimits','keepticks')
hold off
title('V Velocity Fluctuations')
xlabel('Time (min)')
ylabel('Velocity (m/s)')
legend('CSAT 3','CSAT 4')
```

```
%Plot fluctuations for W
Fig.(4);
plot(Time,W1_fluctuation,'r')
xlim([Time(1) Time(end)])
datetick('x','HH:MM','keeplimits','keepticks')
hold on
plot(Time,W2_fluctuation,'b')
xlim([Time(1) Time(end)])
datetick('x','HH:MM','keeplimits','keepticks')
hold off
title('W Velocity Fluctuations')
xlabel('Time (min)')
ylabel('Velocity (m/s)')
legend('CSAT 3','CSAT 4')
%Plot fluctuations for T
Fig.(5);
plot(Time,T1_fluctuation,'r')
xlim([Time(1) Time(end)])
datetick('x','HH:MM','keeplimits','keepticks')
hold on
plot(Time,T2_fluctuation,'b')
xlim([Time(1) Time(end)])
datetick('x','HH:MM','keeplimits','keepticks')
hold off
title('Temperature Fluctuations')
xlabel('Time (min)')
ylabel('Temperature (Degrees C)')
legend('CSAT 3','CSAT 4')
%plots of u'w' and w'T':
```

```
%Begin with fluctuation calculations for u'w' and w'T'
U1W1_fluctuaiton = U1_fluctuation.*W1_fluctuation;
U2W2_fluctuation = U2_fluctuation.*W2_fluctuation;
W1T1_fluctuation = W1_fluctuation.*T1_fluctuation;
W2T2_fluctuation = W2_fluctuation.*T2_fluctuation;
%Plot turbulent momentum flux
Fig.(6);
plot(Time,U1W1_fluctuaiton,'r')
xlim([Time(1) Time(end)])
datetick('x','HH:MM','keeplimits','keepticks')
hold on
plot(Time,U2W2_fluctuation,'b')
xlim([Time(1) Time(end)])
datetick('x','HH:MM','keeplimits','keepticks')
hold off
title('Turbulent Momemtum Flux')
xlabel('Time (min)')
ylabel('u''w'' (m*C/s)')
legend('CSAT 3','CSAT 4')
%Plot sensible heat flux
Fig.(7);
plot(Time,W1T1_fluctuation,'r')
xlim([Time(1) Time(end)])
datetick('x','HH:MM','keeplimits','keepticks')
hold on
plot(Time,W2T2_fluctuation,'b')
xlim([Time(1) Time(end)])
datetick('x','HH:MM','keeplimits','keepticks')
hold off
```

```
title('Sensible Heat Flux')
xlabel('Time (min)')
ylabel('w''T'' (m*C/s)')
legend('CSAT 3','CSAT4')
%calculate covariance and correlation coefficients
covUW1 = cov(Sonic1(:,1),Sonic1(:,3));
rUW1 = corrcoef(Sonic1(:,1),Sonic1(:,3));
covUW2 = cov(Sonic2(:,1),Sonic2(:,3));
rUW2 = corrcoef(Sonic2(:,1),Sonic2(:,3));
covWT1 = cov(Sonic1(:,3),Sonic1(:,4));
rWT1 = corrcoef(Sonic1(:,3),Sonic1(:,4));
covWT2 = cov(Sonic2(:,3),Sonic2(:,4));
rWT2 = corrcoef(Sonic2(:,3),Sonic2(:,4));
%neutral atmospheric conditions
%velocity profile in log layer for CSAT3 (bottom)
z0 = 0.001 ; %roughness, in meters, of conrete base; assuming nearly
perfectly leveled
k = 0.4; %van Karmen constant
V1W1_fluctuation = V1_fluctuation.*W1_fluctuation;
V1W1_avgeragefluctuation = mean(V1W1_fluctuation);
U1W1_avgeragefluctuation = mean(U1W1_fluctuaiton);
u_star = (U1W1_avgeragefluctuation.^2 + V1W1_avgeragefluctuation.^2).^0.25;
%using equation given during lecture
z=linspace(0,2,200);
Ubar = (u_star./k).*log(z./z0); %z/z0 is roughness length
%Plot root mean squared horizontal wind velocity
Fig.(8);
plot(Ubar,z)
hold on
```

```
plot(1.7015,1,'r*')

hold on

plot(1.7730,1.7,'x')

xlabel('Root Mean Squared Horizontal Wind Velocity (m/s)')

ylabel('Height Above Ground (m)')

legend('Log Profile','CSAT 3','CSAT 4')

%average w'T'

W1T1_avgfluc = mean(W1T1_fluctuation);
```

References

Introduction Sources

https://engineering.dartmouth.edu/~d30345d/books/EFM/chap12.pdf
[1] Chapter 12: Atmospheric Boundary Layer. (n.d.). Retrieved February 20, 2016, from https://engineering.dartmouth.edu/~d30345d/books/EFM/chap12.pdf

[2] Obsastro. (2011). Chapter 2- Atmospheric Turbulence "Seeing" Retrieved February 20, 2016, from http://www.ita.uni-heidelberg.de/~dullemond/lectures/obsastro_2011/chap_turb.pdf

[3] Sharman, R. (n.d.). RAL: In Situ Turbulence. Retrieved February 20, 2016, from https://www.ral.ucar.edu/projects/in-situ-turbulence

https://www.ral.ucar.edu/projects/in-situ-turbulence
http://www.ita.uni-heidelberg.de/~dullemond/lectures/obsastro_2011/chap_turb.pdf

[4] Lave, Matthew. "UCSD DEMROES." *UCSD DEMROES*. UCSD, 9 Feb. 2016. Web. 9 Feb. 2016.

[5] "Air Properties." *Air Properties*. Engineering Toolbox, n.d. Web. 19 Feb. 2016.

[6] "NR-Lite Net Radiometer Instruction Manual." *SSRN Electronic Journal SSRN Journal* (n.d.): n. pag. *Campbell Scientific NR-Lite*. Campbell Scientific, Inc. Web. 17 Feb. 2016.